Direct measurements of the energy of intense vorticity filaments in turbulence

J. H. C. Titon and O. Cadot[†]

Laboratoire de Mécanique, Université du Havre, 25 Rue Philippe Lebon, 76058 Le Havre Cedex, France

(Received 24 April 2002; revised manuscript received 17 October 2002; published 18 February 2003)

The global instantaneous power injected in a turbulent shear flow is investigated. A conditional averaging technique reveals the complete energetic transfer scenario of the intense vorticity filaments, which were visualized by Douady, Couder, and Brachet [Phys. Rev. Lett. **67**, 983 (1991)]. It is found that during their existence filaments store a significant part of the turbulent kinetic energy. This energy is dissipated during the destruction phase of filaments. The total energy transferred to small scales due to filaments is quantified on the basis of a global flow visualization.

DOI: 10.1103/PhysRevE.67.027301 PACS number(s): 47.27.−i, 05.40.−a

Small-scale production in turbulence is a major unsolved problem in fundamental physics. Its underlying mechanism is responsible for the large efficiency of turbulent flow in dissipating energy. Turbulence is classically pictured (or stated) as a superposition of structures of different sizes through which energy cascades from large scales to the smallest one. Because of its complexity, theoreticians have to take into consideration some statistical approaches. These do not explicitly account for the dynamic relationship between the different scales, or in other words the process by which the energy is transferred. The experimentalists' approach is difficult because of the high space-time resolution the measurements require. The visualization of turbulent flows, although qualitative, has often proved to be a powerful tool. Observations of the dynamics of vorticity filaments in turbulent boundary layers [1] or in three-dimensional shear flow [2,3] have allowed the authors to suggest a plausible scenario of energy transfer. These rare but intense structures have an evolution similar to vortex breakdown dynamics. Recently, there have been some quantitative characterizations of the pressure in filaments [4–7]. It has been shown [8,9] that filaments participate in the statistical intermittency [10] of the velocity measured at one point. In the present Brief Report, we wish to answer the question: How much do filaments contribute to the mean energy transfer of the total turbulent flow? The definitive way to answer is to measure directly the energy the filaments dissipate, which has, to the best of our knowledge, never been done. Here, we study the total instantaneous power injected into the turbulence when intense vorticity filaments appear in the flow.

In our von Kármán swirl geometry [2–5,7–9,11–13] (Fig. 1), the flow is confined in a cylindrical cell, 19 cm in diameter and 39 cm in height. The turbulence is forced between two enclosed horizontal coaxial counter-rotating Plexiglas stirrers, of radius $R=8.75$ cm and separated by $H=32$ cm. The total volume of fluid is 10.95 l. Each stirrer is composed of a disk fitted with a set of eight regularly disposed vertical blades 6.5 cm long and 1.7 cm high. It is driven individually by a 500 W dc servomotor. The usual definition of the Reynolds number for this experimental setup is

$$\mathrm{Re}=\frac{\Omega R^2}{\nu},$$

where $\Omega/2\pi$ is the rotation frequency of the stirrers of radius R and ν is the kinematic viscosity of the experimental fluid. The turnover time of the experiment is defined as $T=2\pi/\Omega$. We present three experiments for different Reynolds numbers. The first is performed at $\mathrm{Re}=385\,000$ with water at a rotation frequency of 8 Hz. In the second experiment, $\mathrm{Re}=44\,000$, the rotation frequency is still 8 Hz but the kinematic viscosity is 8.75 times larger than the viscosity of water. The fluid used is a water/glycerol 56% mass fraction mixture. Finally, in the third experiment, $\mathrm{Re}=240\,000$, the fluid is water and the rotation frequency is 5 Hz. Referring to [14] the corresponding microscale Reynolds number varies in the range $150<\mathrm{RI}<650$.

Each dc motor is operated at a constant angular velocity by means of tachymetry feedback. The regulation system

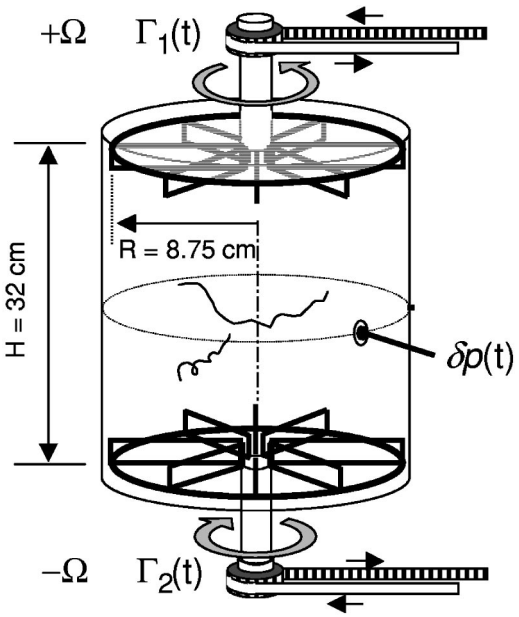

FIG. 1. Experimental cell (see text).

[†]Present address: Laboratoire de Physique et Mécanique des Milieux Hétérogènes de l'Ecole Supérieure de Physique et Chimie Industrielle, 10 Rue Vauquelin, 75 231 Paris Cedex 05, France.

adapts the torque (via a PID control loop) delivered by the motors. The instantaneous torque is measured as an image of the current at the output of the feedback loop. The current is directly proportional to the torque of the motor, following the Laplace law. A torque signal output of 1 V corresponds to 0.52 N m. We deduce the high frequency cutoff f_c of the torque measurements (mainly due to the mechanical system: rotor inertia, transmission belt, disk inertia, etc.) from the angular velocity response of the disk when an angular velocity jump is imposed by the regulation system. The time response is typically 20 ms; thus $f_c = 50$ Hz. Spectral analyses reveal that fluctuations of the turbulent torque occur at frequencies lower than the rotation frequencies $\Omega/2\pi$ (5–8 Hz). The frequency cutoff is then sufficiently high enough and we filter the signals beyond 20 Hz with a *RC* low pass filter. Further details are given in [11]. We denote by $\delta x'$ the variable x centered about the mean and reduced by the rms value: $\delta x' = (x - \langle x \rangle)/\delta x_{\mathrm{rms}}$ with $\delta x_{\mathrm{rms}} = \sqrt{\langle x^2 - \langle x \rangle^2 \rangle}$.

The total power injected by the dc motors during the counter-rotating regime is decomposed into two terms:

$$P^M(t) = P(t) + \Omega(\Gamma_1^S - \Gamma_2^S). \tag{1}$$

The first term $P(t) = \Omega(\Gamma_1(t) - \Gamma_2(t))$ is the total power injected at the large scale of the flow, and $\Gamma_1(t)$ and $\Gamma_2(t)$ are the instantaneous torques on each disk (see Fig. 1). The second term represents the losses that are not due to the flow dissipation (losses due to the bearings, the transmission system, and the watertight joints). They are directly measured when the liquid in the cell is replaced by ambient air (in this case the drag due to the flow is negligible).

The *probability density function* (PDF) of the injected power is shown for the three Reynolds numbers in Fig. 2. Their shapes are similar, showing Gaussian tails with a slightly negative skewness that never exceeds $|s| \leqslant 0.1$. The mean injected power $\langle P \rangle$ follows a scaling law only determined by the inertial parameters as expected by the Kolmogorov K41 theory [11–13], we find

$$\langle P \rangle = 0.31 \rho \Omega^3 R^5, \tag{2}$$

The root mean square value δP_{rms} is found to be

$$\delta P_{\mathrm{rms}} \approx 0.11 \langle P \rangle, \tag{3}$$

whatever the Reynolds number. The coefficient 0.11, which depends on the experimental geometry, is in good agreement with previous measurements in [12], whose authors found 0.1 in a not identical but very similar flow. However, in [12] the skewness is much larger: $s = -0.72$. It is possible that the skewness is more sensitive to the geometric details of the experimental cell than the rms value.

The temporal fluctuations of power are correlated with the appearance of filaments by means of simultaneous wall pressure measurements [4,5]. The pressure transducer (WM106B from PCB Piezotronics®) is localized in the midplane of the cell (see Fig. 1). Figure 2(b) shows the PDF of the pressure fluctuations. The large exponential tail that extends for the negative fluctuations is due to the presence of deep negative peaks in the pressure signal [4]. These peaks are known to be

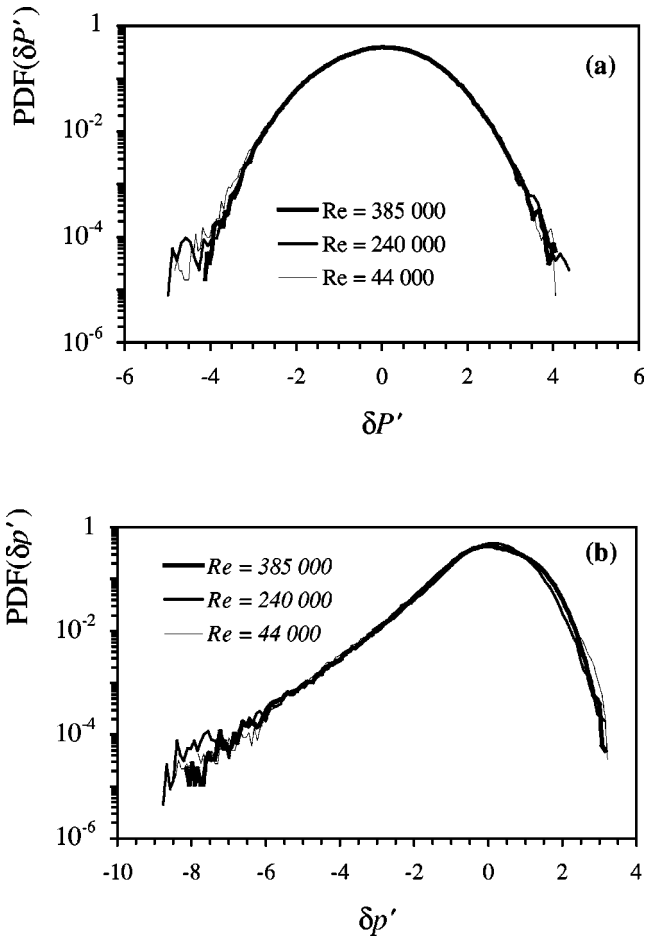

FIG. 2. Probability density function of the nondimensionalized (a) injected power fluctuations and (b) wall pressure fluctuations.

the consequence of intense vorticity filaments passing the pressure transducer [4,5]. The criterion we use for filament detection in the pressure time series is based on a threshold value. If the threshold is too high, some filaments are missed. If the threshold is too low, events due to Gaussian fluctuation are taken into account. A good threshold value will thus optimize the convergence of the subsequent correlation tech-

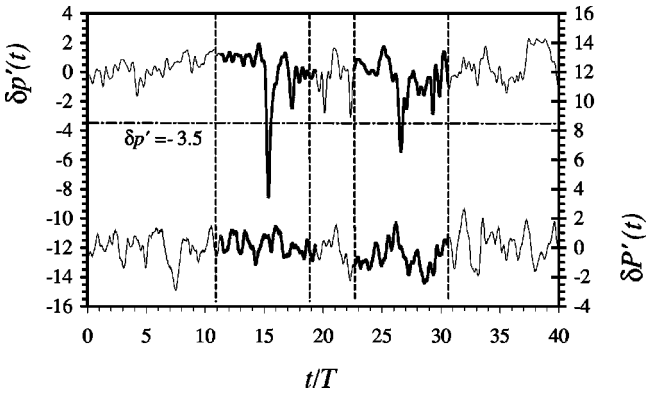

FIG. 3. Sample of simultaneous time series of injected power (bottom) and local wall pressure fluctuations (top). Two windows are selected by the low pressure criterion.

nique. The value is chosen as $\delta p' = -3.5$ (see Fig. 3). A classical peak detector subroutine determines the location t_i of the pressure minima. Once a minimum of pressure is detected at time t_i, a temporal window of duration $[t_i - 4T, t_i + 4T]$ of each signal is recorded. For the three Reynolds numbers, the acquisition duration is 40 min. The analyses detected 344 events for Re=385 000, 397 for Re=44 000, and 245 for Re=240 000. Figure 3 is an example of such recorded time windows. While one selected window alone does not show any clear effect on the power, the conditional average performed over the whole series of detected windows converges to a significant tendency (see Fig. 4).

Figure 4(a) is the low pressure peak average. The asymmetry is related to the filament dynamics. In Refs. [2,3,5], the evolution of the filaments corresponds first to a quick coherent phase during their formation and second to a slower destruction phase similar to vortex breakdown dynamics. Figure 4(b) reveals clearly the total averaged scenario of the power injected during the filament evolution. Its time duration is close to the large-scale turnover time T as previously estimated in [2,3,5] with visualization. The present result gives the quantitative scaling for the filament lifetime as defined in Fig. 4(b): $T_{\text{life}} = 1.2T$.

We can observe three distinct phases in Fig. 4(b). Chronologically, the injected power increases during the first phase. The extra energy supplied feeds the filament formation. The second phase corresponds to an abrupt decrease of the injected power during the time T_{life}. The amplitude of this decrease corresponds to $0.8\delta P_{\text{rms}}$. This value is surprisingly large because it is comparable to the typical fluctuation of the injected power δP_{rms}. Referring to Eq. (3), the power decrease represents 8.8% of the mean power injected into (or dissipated by) the global flow. The kinetic energy that has been accumulated during the formation is actually stored during the time duration T_{life}. During the third phase, the filaments are destabilized; the coherent energy is then transferred to smaller scales with no coherence. The power injected increases during this dissipative process.

We compute the nondimensional kinetic energy of the filament versus time as

$$\delta\varepsilon(t/T) = \int_0^{t/T} \delta P'(\tau)\, d\tau - \delta\varepsilon'_{\text{mm}}. \tag{4}$$

We take as zero the minimum of this energy. The kinetic energy is shown in Fig. 4(c). The maximum energy of the filament is close to $\delta\varepsilon'_{\text{max}} \approx 0.4$ whatever the Reynolds number. The dimensional energy of the filament is

$$\delta\varepsilon_{\text{max}} = T\,\delta P_{\text{rms}}\,\delta\varepsilon'_{\text{max}}. \tag{5}$$

Including Eq. (3) we obtain

$$\delta\varepsilon_{\text{max}} \approx 0.044\langle P\rangle T. \tag{6}$$

Hence, the kinetic energy accumulated by a filament is equal to 4.4% of the total energy injected in the flow during one turnover time. An essential point to know is how many filaments appear in the bulk of the flow per unit of turnover time. We count at least one filament per turnover time using the same visualization technique as in [2,3,5]. We can conclude that more than 4.4% of the total injected energy is transferred to the small scales by the vorticity filaments. We underline that the counting of the number of filaments is possibly underestimated since some are missed due to the great difficulty of volume visualization.

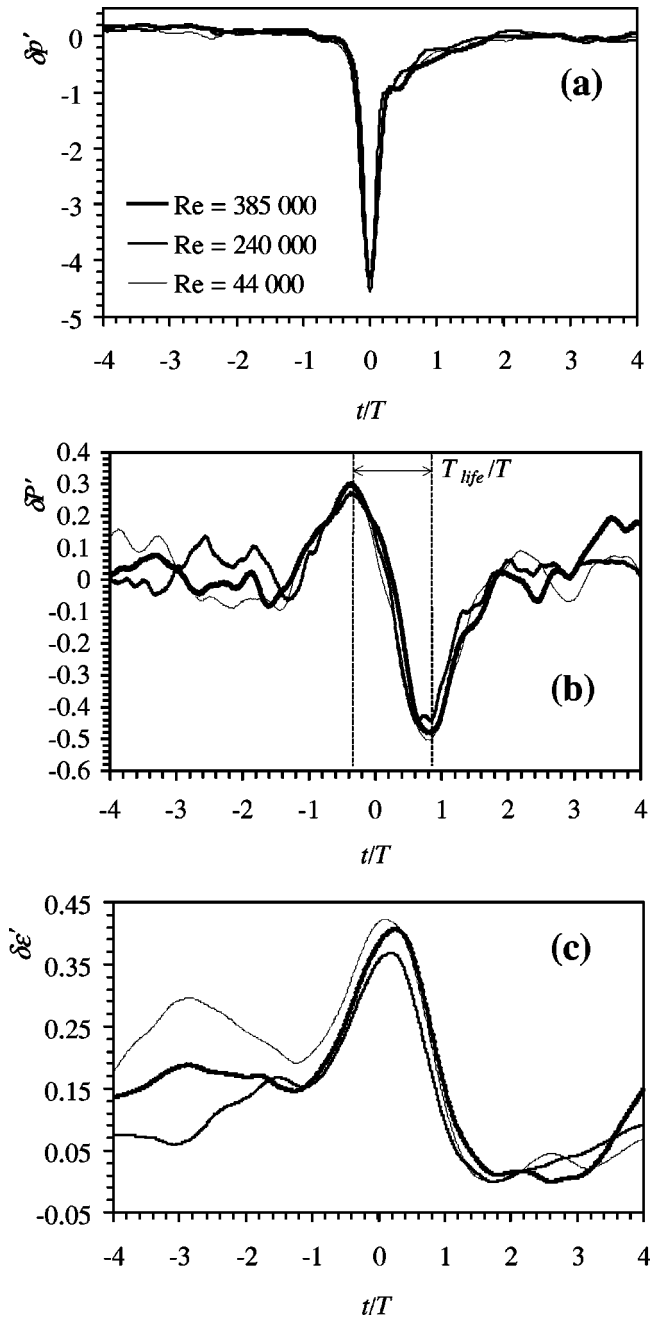

FIG. 4. Conditional average by low pressure detection of (a) the pressure time series and (b) the injected power time series. (c) is the energy computed from (b) (see text).

From Figs. 2(a) and 2(b) or 4(a), 4(b), and 4(c), we cannot distinguish any dependency on the Reynolds number. We deduce that neither the time interval of transfer nor the kinetic energy stored by the filament depends on the viscosity. The filament dynamics thus belong to the inertial range scale

of the turbulence. This suggests that the filament core size does not depend on the viscosity. It is established [5] that filaments result from a process of stretching that concentrates the vorticity in a tubelike form. If the mechanism remains stable, the vorticity concentration process is stopped by viscosity and the core size results from a balance between stretching and viscous diffusion [15]. However, no clear scaling of the filament core size has been measured in turbulent flows yet. The present experimental results indicate that the filaments are destroyed before an ultimate viscous limit is reached. This point is in good agreement with the mechanism proposed by Le Dizès *et al.* [16]. In their theoretical study they show how stretching can stabilize the three-dimensional instability of initially bidimensional vortices. Although filaments are stretched vortices, they argue that filaments can be destroyed by elliptical instability during their formation process. This instability is released if the stretching is not maintained great enough to counteract the destabilizing effect of the strains due to the turbulent fluctuation. Two possible mechanisms could affect the stretching during filament formation. The first is simply related to the time coherence of the stretching field. This field is produced by the large-scale structures of the turbulence [5] and has a correlation time comparable to one turnover time. The second mechanism is related to the recent investigation [17] involving the interaction between stretching and vorticity. The feedback effect of fast rotation produces a two-dimensionalization that reduces the stretching in the filament core.

In conclusion, the complete scenario of the energetic transfer of filaments is identified. A plausible scenario is the following. Some energy is first extracted from the large-scale structures to produce stretching in which the vorticity is concentrated. Secondly, the filament stores its kinetic energy during a time interval $T_{\mathrm{life}}=1.2T$. Thirdly, the filament is finally destroyed through a violent explosion while its energy is transferred with no coherence to smaller scales. This destruction aborts the concentration process of vorticity before the core size can reach the viscous limit. On the basis of global visualization together with energy measurements, it may be predicted that, although they are rare events, filaments could be responsible for a significant part of the mean turbulent energy transfer. However, some further investigations are necessary to count exactly the number of filaments. This could be achieved [18] by a wavelet analysis of the global power time series using as analyzing wavelet Fig. 4(b).

LPMMH de l'ESPCI is UMR 7636 of the CNRS. The authors are grateful to P. Petitjeans for his critical reading of this manuscript. O.C. would like to thank the CNRS for facilitating his integration to the Laboratoire de Physique et Mécanique des Milieux Hétérogènes de l'Ecole Supérieure de Physique et Chimie Industrielle.

[1] H. T. Kim, S. J. Kline, and W. C. Reynolds, J. Fluid Mech. **50**, 33 (1971).
[2] S. Douady, Y. Couder, and M.-E. Brachet, Phys. Rev. Lett. **67**, 983 (1991).
[3] S. Douady and Y. Couder, in *Turbulence in Extended Systems*, edited by R. Benzi, C. Basdevant, and S. Ciliberto (Nova Science, Commack, NY, 1993), p. 3.
[4] S. Fauve, C. Laroche, and B. Castaing, J. Phys. II **3**, 271 (1993).
[5] O. Cadot, S. Douady, and Y. Couder, Phys. Fluids **7**, 630 (1995).
[6] E. Villermaux, B. Sixou, and Y. Gagnes, Phys. Fluids **7**, 2008 (1995).
[7] A. La Porta, Greg A. Voth, F. Moisy, and Eberhard Bodenschatz, Phys. Fluids **12**, 1485 (2000).
[8] O. Cadot, in *Small-Scale Structures in Three Dimensional Hydro and Magneto-Hydrodynamic Turbulence*, Vol. 462 of *Lecture Notes in Physics*, edited by M. Meneguzzi, A. Pouquet, and P.-L. Sulem (Springer-Verlag, Berlin, 1995), p. 89.
[9] P. Chainais, P. Abry, and J.-F. Pinton, Phys. Fluids **11**, 3524 (1999).
[10] F. Anselmet, Y. Gagne, E. J. Hopfinger, and R. A. Antonia, J. Fluid Mech. **140**, 63 (1984).
[11] J. H. Titon and O. Cadot, Phys. Fluids (to be published).
[12] R. Labbé, J.-F. Pinton, and S. Fauve, J. Phys. II **6**, 1099 (1996).
[13] O. Cadot, Y. Couder, A. Daerr, S. Douady, and A. Tsinober, Phys. Rev. E **56**, 427 (1997).
[14] H. Willaime, F. Belin, and P. Tabeling, Eur. J. Mech. B/Fluids **17**, 489 (1998).
[15] H. K. Moffatt, S. Kida, and K. Ohkitani, J. Fluid Mech. **259**, 241 (1994).
[16] S. Le Dizès, M. Rossi, and H. K. Moffatt, Phys. Fluids **8**, 2084 (1996).
[17] B. Andreotti, S. Douady, and Y. Couder, J. Fluid Mech. **444**, 151 (2001).
[18] A. Arnéodo (private communication).